

# Segmented flow reactor for synthesis of quantum dot nanocrystals and plasmonic nanoparticles

R C Mbwanche<sup>1</sup>, L B Matyushkin<sup>1</sup>, O A Ryzhov<sup>1</sup>, O A Aleksandrova<sup>1</sup>, V A Moshnikov<sup>1,2</sup>

<sup>1</sup>St. Petersburg State Electrotechnical University “LETI”, Pr. Popova 5, St. Petersburg, 197376 Russia

<sup>2</sup>Peter the Great St. Petersburg Polytechnic University, Polytechnicheskaya, 29, St. Petersburg, 195251, Russia

**Abstract.** This research presents an automated method of synthesizing semiconductor and metal nanoparticles using flow reactor synthesis as a new alternative to the batch method of synthesizing nanoparticles. Experiments were carried out to determine the optimal flow rates of reagents droplets. The reactor was successfully applied to the synthesis of colloidal solutions of semiconductor (CdSe) and metal (Ag) nanoparticles. This instrument is applicable both in material science laboratories and in industry.

## 1. Introduction

The most popular method for the synthesis of monodisperse semiconductor nanoparticles is the hot injection method, proposed by the Bawendi group in 1993 [1]. However, this technique is performed in a chemical flask, which prevents the technology from scaling to the industrial level and leads to high market price of such nanoparticles. This was the cause for the flow reactor synthesis [2] as a technology that allows large-scale automated production and at the same time offers such benefits as better control of the heat and mass transfer, better precision of the cooling rate, and reproducibility. The flow synthesis allows monitoring parameters and spending reagents more efficiently than the traditional chemical synthesis [3].

There are two major types of flow reactors used in the synthesis of quantum dots; continuous and segmented flow. In continuous flow reactors, reaction and precipitation occur in the same phase. Miscible streams of reagents are injected into the channel where they mix and react. This has been used to produce high quality nanoparticles like metals [4], metal oxides [5] and compound semiconductors [6]. However, the liquid front experiences friction with the walls of the channel which induces a parabolic velocity profile across the channel with particles contacting the walls of the channel having greater resident time compared to particles located at the center figure 1. This variation of speed leads to polydisperse size distribution. Also over time, due to contact with the channel walls, precipitating particles begin to accumulate and form a stagnant layer adjacent to the channel walls leading to eventual fouling of the channel.



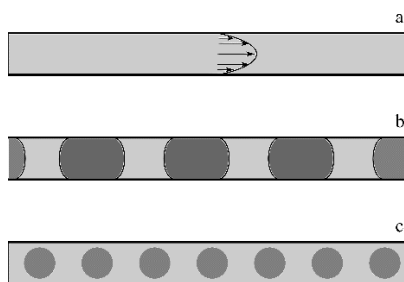


**Figure. 1.** The diagram illustrating continuous (a) and segmented (b, c) modes of flow in channels with a circular cross section

In contrast to continuous flow microractors, for a segmented flow reactor, an additional immiscible fluid is also injected at the same time with the reagents. This carrier fluid splits and surrounds the reacting mixture forming tiny droplets, which flows through the channel. Inside the droplets, a uniformly circulating flow profile develops providing a completely uniform residence time for the nanoparticles and an enhanced mixing of reagents. [7]. The carrier fluid can be gas as in the case of “gas/liquid” mode or a liquid as in a “liquid/liquid” mode. Although the “gas/liquid” mode prevents the parabolic velocity flow profile, the mixing reagents droplets continue to make contact with the channel walls, eventually leading to channel blockage. These challenges, however, are eliminated by the “liquid/liquid” mode as it not only provides an equal residence time within a droplet, but it also isolates the droplets from the walls of the channel by wetting the full length of the channel wall. This is better achieved when the carrier phase is in excess.

Segmented flow reactor was first used to synthesize nanocrystal at room temperature [8]. However, in order to increase particle crystallinity there is a need to synthesize nanocrystal at higher temperature. Chan et al. in 2005 synthesized CdSe quantum dots [9] and after a recorded period of five hours the surface coating of the channel wall began to degrade rapidly resulting in an irregular flow. Later on, using the same reagent and carrier liquid Nightingale et al. developed a more robust segmented flow reactor using polytetrafluoroethylene polymer with the ability to withstand temperature to about 250 °C, beyond which the polymer starts to degrade [10].

Like stated above, flow reactor allows large-scale automated production. Scaling out is rather simpler than in batch reaction since it does not require changing the reactor geometry and also although the material throughput increases, the chemistry is the same. This can be achieved by operating large numbers of identical reaction channels in parallel [11]. Notable success was recorded using five-channel droplet-based microreactor to synthesize CdSe [12]

Recently there have been improvements of flow reactor aiming at widening the range of materials and chemistries to which it can be used. The one-step procedure, in which all reagents are loaded into the droplets at the outset, limits the range of materials that can be used. However, the multistep droplet reactor allows reagents to be sequentially added into the flowing droplets as the reaction proceeds. The report [13] shows a three-phase system which involves a gas phase and two immiscible liquids.

In our research work, however, we developed a high temperature, two-phase segmented flow reactor using polytetrafluoroethylene (PTFE) capillary channel. The reactor is of a modular construction with: isolated temperature zones in order to separate nucleation and growth of particles, a passive generation of droplets and a compact for primary diagnosis of the nanocrystals.

## 2. Flow reactor design development

The working principle is such that precursors A and B and the carrier liquid C which are contained in three separate syringes are squeezed out at a predetermined speed using three syringe pumps, figure 2. The liquids go into the mixing cell, where a droplet flow of precursor solution in the carrier medium is formed. This total flow moves through the capillary (inner diameter 800 μm), passing through two zones with different temperatures:  $T_n$  is the temperature corresponding to nanocrystal nucleation and  $T_g$  is the temperature of the nanoparticles growth. The final stage is the selection of colloidal solutions of nanoparticles and their primary diagnosis by the compact spectrophotometer.

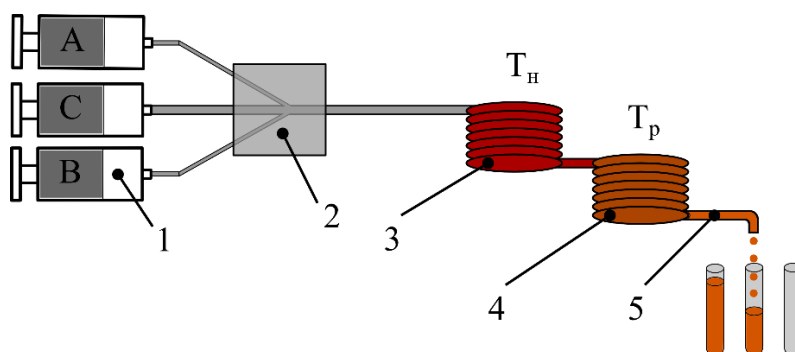


**Figure 2.** Schematic diagram of the installation: 1 — syringe pumps, 2 — mixing module, 3 — nucleation module, 4 — growth module, 5 — selection of nanoparticles

The whole device is operated with the help of a microcontroller Arduino Mega 2560 and a personal computer with special software developed in NI LabVIEW [14]. The program sets the required flow rates and temperatures of nucleation and growth zones. With this design we were able to isolate the various processes; mixing, precipitation process, nucleation and growth. Also we used a transparent PTFE polymer, which enabled us directly observe and precisely control the whole process of the synthesis.

One of the important factors for obtaining the monodisperse nanoparticle in droplet form is a stable flow rate control system. The flow rate control system consists of syringe pumps which are of modular construction, stepper motor and the transmission system which was fabricated using a 3D-printer. The precursors and the carrier liquid are ejected from the syringe pumps using a stepper motor. Due to the need for a relatively low flow rates of the liquid, in our previous work we used a cylindrical gear transmission with a transfer coefficient of six. However, at very low flow rate the motors began to vibrate. The pump design together the software program was therefore modified, replacing the gears with belt having a transfer coefficient of four and the minimum flow rate of 1.5 l / sec.

Although we achieved a minimum flow rate that favour the formation of droplet, there was a need for turbulence at the onset of the reaction before the droplets are formed in order to maximise mixing of the reagent. Three basic structure were proposed; flow-focusing figure 3a, Y-shape, figure 3b and T-type figure 3c microchannel. So as to include the carrier fluid we constructed a device, figure 4, which is a modification of the Y-shape microchannel to enhance mixing, preceding the formation of droplet. This in fact was an important objective of the pump design

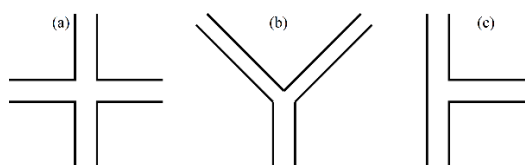


**Figure 3.** Microchannel for nanoparticle precipitation: (a) flow focusing microchannel; (b) Y-shaped microchannel; and (c) T-type microchannel

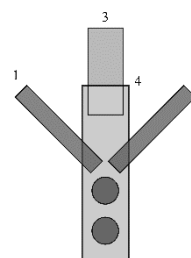


**Figure 4.** Schematic picture of the device for forming droplets: 1,2– reagents inlet, 3– carrier fluid inlet, 4– microreactor channel

The production of monodisperse colloids requires a temporally discrete nucleation event followed by slower controlled growth on the existing nuclei[15]. While particle size depends on the duration of the growth phase, which is regulated by the flow rate and the number of capillary loops in the growth module. We separated this stages in order to control have a precise control on the synthesis. The main elements for temperature control system are heating element, and oil bath in which is immersed a platinum thermal resistance temperature detector that measures the temperatures  $T_n$  and  $T_g$ . The heat from the heating element is transferred to a beaker made of heat-resistant glass filled with liquid with a high boiling point, in which a part of the capillary is immersed.

### 3. Result

To determine the optimum flow rates for precursors mixing and the formation of the “liquid/liquid” flow, we used water-based inks as model precursors and hexane as the carrier liquid as reported in the report [16], figure 5. According to the results, it can be assumed that the optimum flow rate range for three streams, when the precursors are completely mixed and the carrier liquid flow divides into droplets, is in the range 10–50  $\mu\text{l/s}$ . It is important to note that different pairs of liquids require another assessment.

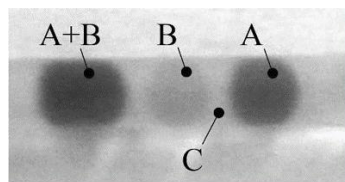


**Figure 5.** Flow elements in the PTFE capillary: A and B – modelling precursors, C – carrier fluid

Figure 6 shows the results of the experiment, in which all flow rates equally varied  $v_A = v_B = v_C$ . The smaller the flow rates, the smaller the droplet size of mixed precursors, but at a rate of 1,2  $\mu\text{l/s}$  the precursor flows do not mix uniformly (color of drops changes). At the same time, too high speed causes the transition of flow shape to laminar. These results suggest that the best speed is in the range 10–20  $\mu\text{l/s}$

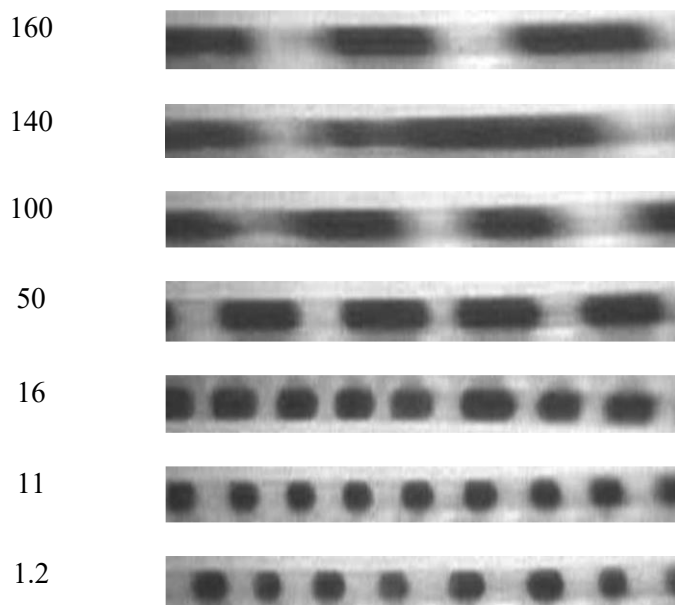


**Figure 6.** Evolution of the shape of the segmented flow with a simultaneous change of the flow rates ( $\mu\text{l/s}$ ) precursor A, B and C of the liquid medium

### 3.1. Metal Nanoparticles Synthesis

The synthesis of metal nanoparticles was carried out using the example of silver nanoparticles. The source of the silver ions (liquid A) is a solution of silver nitrate  $\text{AgNO}_3$ , a solution of ascorbic acid and sodium citrate was used as a reductant and stabilizer (liquid B). The carrier (liquid C) was toluene. The synthesized particles have strongly pronounced plasmon resonance Figure 7. Compared with results in [17], it can be assumed that synthesizing nanoparticles have a diameter of 25–30 nm with the assumption that all particles are spherical.

### 3.2. Semiconductor Nanoparticles Synthesis

The synthesis of semiconductor nanoparticles was tested on CdSe nanoparticles in aqueous medium, where liquid A was a  $\text{NaHSe}$  solution ( $\text{Se}^{2-}$  precursor), B –  $\text{CdCl}_2$  ( $\text{Cd}^{2+}$  precursor) and L-cysteine (a stabilizer of nanoparticles), C – dodecane. Position of the first exciton peak in the absorption spectrum moved to longer wavelengths as the growth of the particles Figure 8. From the absorption spectrum of the synthesis, average diameters of the nanoparticles were found using the formula from [18]: 1 min – 1.4 nm and 15 min – 1.8 nm.

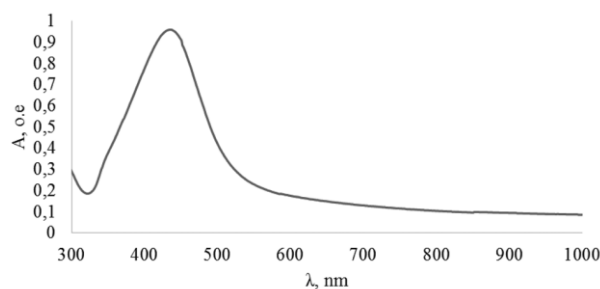


**Figure 7.** The spectrum of the optical density for silver nanoparticles

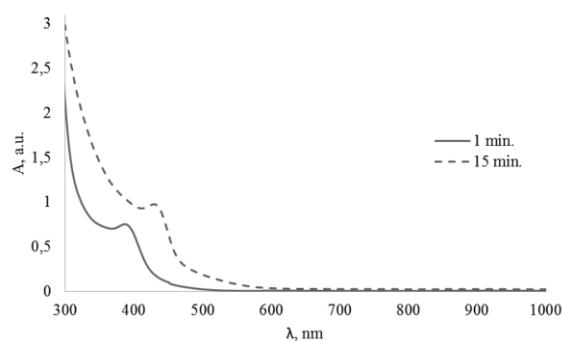


**Figure 8.** The spectrum of the optical density for CdSe nanoparticles with different growth time

## 4. Conclusions

The study developed a laboratory model of the flow reactor system for the synthesis of nanoparticles. The proposed technique involving syringe pumps allows creating a segmented stream with precision control. It is shown that using the proposed hardware solution, it is possible to synthesize semiconductor and metal nanoparticles in the aqueous medium. From the absorbance spectra, particle sizes were defined for Ag it is about 25–30 nm, and in the case of CdSe – 1,4 and 1,8 nm for 1 and 15 min. of growth respectively. The obtained nanoparticles were used in studies [20, 21] as a replacement for traditional biomarkers (phosphors) in biology and medicine

## Acknowledgments

The research was carried out under a grant from the Russian Research Foundation (project 14–15–00324).

## References

- [1] Murray C B, Norris D J and Bawendi M G 1993 *J. Am. Chem. Soc.* **115**(19) 8706 reference
- [2] Nakamura H, Yamaguchi Y, Miyazaki M, Maeda H, Uehara M and Mulvaney P 2002 *Chem. Commun.* **23** 2844
- [3] Pan J, El-Ballouli A O, Rollny L, Voznyy O, Burlakov V M, Goriely A and Bakr O M 2013 *ACS nano* **7**(11) 10158 r reference
- [4] Song Y J, Henry L L and Yang W T 2009 *Langmuir* **25** 10209–117
- [5] Miyake T, Ueda T, Ikenaga N, Oda H and Sano M 2005 *J. Mater. Sci.* **40** 5011–13
- [6] Edel J B, Fortt R, deMello J C and deMello A J 2002 *Chem. Commun.* 1136–37

- [7] Chan E M, Alivisatos A P and Mathies R A 2005 *J. Am. Chem. Soc.* **127** 13854–61
- [8] Shestopalov I, Tice J D and Ismagilov R F 2004 *Lab Chip* **4** 316–21
- [9] Chan E M, Alivisatos A P and Mathies R A 2005 *J. Am. Chem. Soc.* **127** 13854–61
- [10] Nightingale A, Krishnadasan S H, Berhanu D, Niu X, Drury C, McIntyre R, Valsami- ones E and de Mello J C 2011 *Lab Chip* **11** 1221–7
- [11] Phillips T W, Ioannis G L, and Richard M M 2014 *Lab on a Chip* **14**(17) 3172-80
- [12] Nightingale A, Bannock J H, Krishnadasan S H, O'Mahony F T F, Haque S A, Sloan J, Drury C, McIntyre R and de Mello J. C, 2013 *J. Mater. Chem. A* **1**, 4067
- [13] Nightingale A M., et al 2014 *Nature communications* **5**
- [14] Ryzhov O A, Matyushkin L B 2015 *JPCS* **643** 012016
- [15] Overbeek JThG 1982 *Adv. Coll. Int. Sci.* **15** 251–77
- [16] Aleksandrova O A, Moshnikov V A, Matyushkin L B, Mbwanche R, and Ryzhov O A 2015 *Humanities and Science University Journal* **15** 13–21
- [17] Pal S, Tak Y K, Song, J M 2007 *Appl. Environ. Microbiol.*, **73**(6), 1712
- [18] Yu W W, Qu L, Guo W, Peng X J 2003 *Chem. Mater.* **15**(14), 2854